Quantum Information & Quantum Computing

(Experimental Part)

Oliver Benson
SoSe, 2016

Contents

1 Introduction **5**

2 Optical and Cavity QED Implementations **7**
2.1 Properties of an optical quantum computer 7
2.1.1 Single Quantum Gates for Photons 7
2.1.2 Photon-Photon-Interaction 9
2.2 Quantum Computation with Linear Optics 11
2.2.1 Hong-Ou-Mandel Interference 11
2.2.2 The KLM-Gate 13
2.2.3 Another intuitive two-photon gate 15
2.2.4 Experimental demonstrations 16
2.2.5 Scalability of LOQC 17
2.2.6 Summary: Optical photon quantum computer 19
2.3 Cavity Quantum electrodynamics 20
2.3.1 Jaynes-Cummings-Hamiltonian 20
2.3.2 Resonant Interaction 22
2.3.3 Off Resonant Interaction/Phase Shifts 27
2.3.4 Flying Qubits 30
2.3.5 Summary: Cavity QED implementation of quantum computers 33

3 Ion Trap Implementations **34**
3.1 Trapping Ions 34
3.1.1 Paul traps 34
3.1.2 Trapping ion strings 37
3.1.3 Normal Modes 40
3.2 Laser Cooling 42
3.2.1 Doppler Cooling 43
3.2.2 Harmonic potential 44
3.2.3 Sideband Cooling 44
3.2.4 Choosing atoms 45
3.3 Single and Two Qubit Gates 47
3.3.1 Hamiltonian of ions in a trap 47
3.3.2 Interaction with a laser field 47
3.3.3 Single qubit operation 49
3.3.4 Two qubit operation 50
3.4 Experimental Realization of a CNOT Gate 51
3.5 Gates and Tricks with Single Ions 56
3.5.1 Demonstration of Deutsch-Jozsa 56
3.5.2 Teleportation of atomic qubits 57
3.5.3 A Quantum Byte 60
3.5.4 Novel Trap Designs 62

3.6 Ion trap Cavity QED Systems 68
3.7 Summary: Ion trap implementation of quantum computers . . . 72

4 Solid State Implementation of Quantum Computers 73
4.1 Superconducting Qubits 73
4.2 Josephson Charge Qubits 73
4.2.1 Single qubit gates 73
4.2.2 Experimental Results on Single qubit rotation: 76
4.2.3 Two-qubit gates 81
4.3 Josephson Flux Qubits 82
4.4 Readout of Josephson Qubits with SETs 83
4.5 Silicon-based Quantum Computation/Spintronics 87
4.5.1 Single qubit gates 88
4.5.2 Two-qubit gates 90
4.5.3 Single spin measurement 91
4.6 Quantum Dots as Qubits 94
4.6.1 Fabrication of quantum dots: 95
4.6.2 Single qubit gates: 98
4.6.3 Two-qubit gates: 100
4.6.4 Initialization and read-out 100
4.6.5 Optical manipulation of quantum dots 101
4.7 Summary: Solid State Implementation 106

dummy

1 Introduction

Some requirements for the physical implementation of quantum computation (according to David DiVincenzo, Fortschr. Phys. **48**, 9-11, p. 771 (2000)):

1. *A scalable physical system with well characterized qubits.*
   As discussed above a qubit could be encoded in any two different quantum states. Examples are given in the following. The main consideration is wether the step from 2 qubits to n qubits is possible. This situation may be compared to the first implementations of classical computers:
   The first machines made from electro-mechanical (Zuse Z1 1938) and later electrical subunits (electrical tubes, IBM 1948) could have been scaled up in principle to increase the computer's power. But, realistically the failure probability and also the energy consumption would have scaled as well. Only the invention of the semiconductor based subunits made scaling feasible.

2. *The ability to initialize the state of the qubits to a simple initial state, such as* $|0, 0, ...0\rangle$.
   In almost all of the above described algorithms initialization is a first step. This initialization may be easy for some physical systems, but crucial for others. If the qubit is encoded in two bits, say with an energy difference ΔE then initialization can be accomplished by cooling to below $T << \Delta E/k_b$. This thermal relaxation of the qubits may take too long a time for a computation. Active initialization may be required.

3. *Long relevant decoherence times, much longer than gate operations.*
   Decoherence is crucial for any quantum computation. It transforms pure states in statistical mixtures and destroys entanglement. The problem of decoherence is the more difficult the larger the quantum system gets: *We do not observe quantum objects in our classical world!* The issue that decoherence must be negligible as long as the computation takes was considered the main obstacle in quantum computation. The suggestion of quantum error correcting codes (Shor 1995) demonstrated that this is *not* the case! Error correcting codes and fault tolerant computation make arbitrary long calculations possible as soon as the decoherence is negligible for about $10^4 - 10^5$ clock times. This is still a very stringent requirement. The price one has to pay is to have each qubit encoded with 3-10 additional qubits for error correction, which then requires even more complex systems.

4. *A universal set of quantum gates.*
   A set of universal gates consists e.g. of single qubit operations and a $CNOT$ gate. Gates are unitary operators. In some systems no appropriate

gates may be constructed easily. Interaction between qubits may influence not only one or two, but many other qubits. Interactions can not be switched on and off arbitrarily and can not be controlled with arbitrary precision.

5. *A qubit-specific measurement capability.*
   It is not easy in some systems to perform a measurement with 100% precision. However, this is less of a problem, since the computation may be repeated several times. (If a detection works only with 90%, then a three times repetition already gives 97% fidelity).

For quantum computation the first 5 requirements suffice, but in a wider context of quantum information processing or networking two more features would be desirable:

1. *The ability to interconvert stationary and flying qubits.*
2. *The ability to faithfully transmit flying qubits between specific locations.*

The notation "flying" qubits was introduced by Kimble. It refers to photons which should be the ideal long-distance carriers for quantum information. The use of the well developed optical fiber communication system would be a tremendous advantage. However, transport (although over relatively short distances) is also discussed in some solid-state implementation of quantum computers.

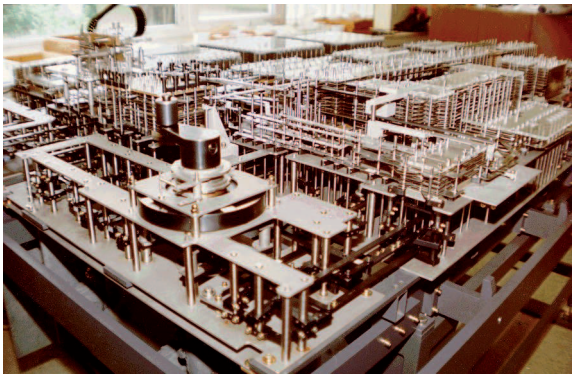

Figure 1: Some details of the Zuse Z1 (Berlin Technical Museum)

The above mentioned items will be discussed from the viewpoint of the different systems introduced in the following section. To summarize:
There is no fundamental physical problem to build an arbitrary large quantum computing device.

2 Optical and Cavity QED Implementations

2.1 Properties of an optical quantum computer

2.1.1 Single Quantum Gates for Photons

Single photons can represent qubits. The advantage of using photons is that they are easy to produce and to detect with high efficiency. A qubit is usually represented with two optical modes:

$$|1\rangle = |1\rangle_1 |0\rangle_2 = |10\rangle = \text{one photon in mode one, zero photons in mode two or}$$
$$|0\rangle = |0\rangle_1 |1\rangle_2 = |01\rangle = \text{one photon in mode two, zero photons in mode one}$$

This representation of qubits is called the *dual-rail representation.* The free time evolution of the qubits is given by the Hamiltonian:

$$H = \hbar\omega a^\dagger a$$

where $a^\dagger$ and a are the creation and annihilation operators for a photon. The free evolution thus only adds an overall phase which can be neglected.

The modes can be two physically separated modes (two "beams") or two modes with orthogonal polarization (horizontal and vertical). Single qubit gates can very easily be realized with the help of linear optical elements (mirrors, phase shifters, beam splitters).

Two ways to encode a qubit (two polarizations or two spatial modes) can be easily exchanged.

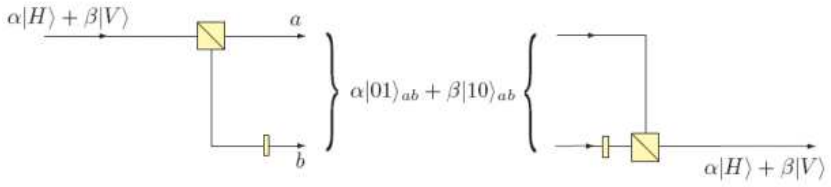

Figure 2: Transfer of polarization encoding into encoding via two spatial modes and vice versa [Myers and Laflamme, arXiv:quant-ph/0512104 v1 13 Dec 2005]

A *mirror* is used to redirect beams and arrange networks. Low loss mirrors with 99.9% reflectivity are obtainable.

A *phase shifter* is a slab of transparent (low loss) material with index of refraction n. It simply retards one optical mode with respect to the other. Its action is described as:

$$\begin{aligned} R_z(\Delta) &= \exp(-i\sigma_3\Delta/2) \\ \text{with the Pauli matrix } \sigma_3 &= \begin{pmatrix} 1 & 0 \\ 0 & -1 \end{pmatrix} \text{ and } \Delta = (n-n_0)L/c_0 \end{aligned}$$

The phase shift Δ is defined by the different optical paths through the material of length L. The following gives a graphical representation of the phase gate where the upper wire corresponds to the state $|0\rangle = |01\rangle$ and the lower wire to the state $|1\rangle = |10\rangle$:

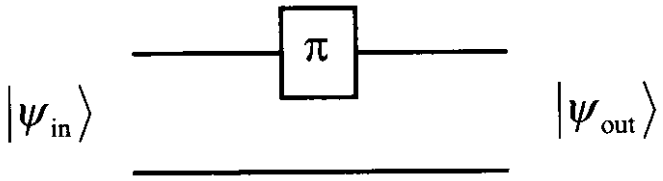

Figure 3: Graphical representation of a phase gate

A *beam splitter* is a piece of transparent (low loss) material with a thin metal coating.

A beam splitter acts on two modes which can be described by annihilation and creation operators $a, a^\dagger$ and $b, b^\dagger$, respectively. There is a transformation between creation/annihilation operators before (subscript 0) and after (subscript 1) a beam splitter with a reflectivity of $R = \cos^2\theta$ as follows (e.g., for the annihilation operators):

$$\begin{pmatrix} a_1 \\ b_1 \end{pmatrix} = \begin{pmatrix} \cos\theta & \sin\theta \\ -\sin\theta & \cos\theta \end{pmatrix} \begin{pmatrix} a_0 \\ b_0 \end{pmatrix}$$

Thus, with e.g. the state $|\Psi_{in}\rangle = |0\rangle = |01\rangle = b_0^\dagger|00\rangle$ as input the output is

$$|\Psi_{out}\rangle = (\sin\vartheta a_1 + \cos\vartheta b_1)|00\rangle = \cos\vartheta|01\rangle + \sin\vartheta|10\rangle$$

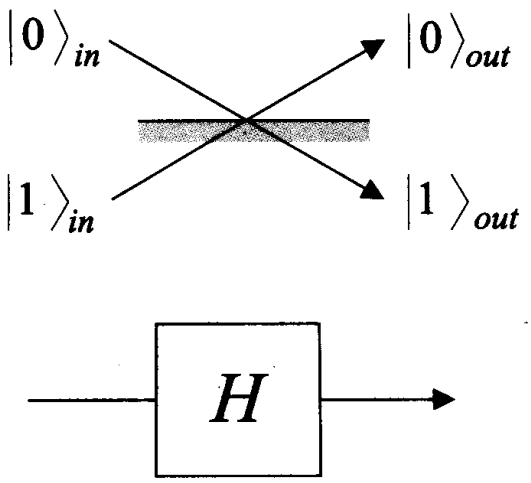

Figure 4: Schematics of a beam splitter

or with the state $|\Psi_{in}\rangle = |1\rangle = |10\rangle = a_0^\dagger |00\rangle$ as input the output is

$$|\Psi_{out}\rangle = (\cos\vartheta a_1 - \sin\vartheta b_1)|00\rangle = \cos\vartheta |10\rangle - \sin\vartheta |01\rangle$$

The beam splitter together with a π-phase shifter acts (up to an overall phase) as a Hadamard gate.
Phase shifters and beamsplitters thus allow the construction of arbitrary single qubit gates!

2.1.2 Photon-Photon-Interaction

The main obstacle of optical quantum computation is to realize controlled gates which require a qubit-qubit (therefore a photon-photon) interaction. Interaction between photons can be established inside certain non-linear materials. Non-linear effects are rather weak. Strongest non-linearities are usually achieved close to resonances which then means a pronounced absorption as well. One type of non-linear material leads to the **Kerr-Effect.** The Kerr-Effect is described by the following Hamiltonian:

$$H_{Kerr} = -\chi a^\dagger a b^\dagger b$$

After propagation through some Kerr material of length L it corresponds to a transformation K:

$$K = \exp(i\chi L a^\dagger a b^\dagger b)$$

K acts on the basis states $|00\rangle$, $|01\rangle$, $|10\rangle$, and $|11\rangle$ as follows:

$$\begin{aligned} K|00\rangle &= |00\rangle \\ K|01\rangle &= |01\rangle \\ K|10\rangle &= |10\rangle \\ K|11\rangle &= \exp(i\chi L)|11\rangle \end{aligned}$$

If a huge Kerr effect is achieved with $i\chi L = i\pi$ and thus $K|11\rangle = -|11\rangle$ then a CNOT can be constructed, because CNOT can be factorized as:

$$U_{CN} = (I \otimes H)K(I \otimes H)$$

where

$$(I \otimes H) = \begin{pmatrix} 1 & 1 & 0 & 0 \\ 1 & -1 & 0 & 0 \\ 0 & 0 & 1 & 1 \\ 0 & 0 & 1 & -1 \end{pmatrix} \quad \text{and} \quad \text{K=} \begin{pmatrix} 1 & 0 & 0 & 0 \\ 0 & 1 & 0 & 0 \\ 0 & 0 & 1 & 0 \\ 0 & 0 & 0 & -1 \end{pmatrix}$$

The following figure shows a possible realization of a Kerr-gate using dual-rail representations of single photon qubits: The presence of light (single photon) in mode s produces a phase shift in one interferomter arm, thus sending a photon to dector D1 and D2, respectively.

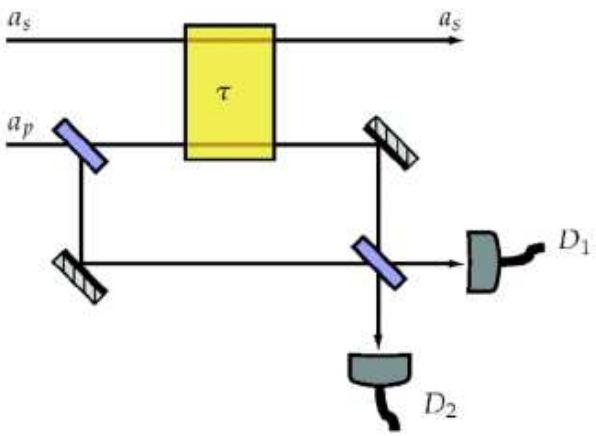

Figure 5: Schematics of a Kerr-gate

2.2 Quantum Computation with Linear Optics

2.2.1 Hong-Ou-Mandel Interference

Recent proposals suggest a strong photon-photon interaction without using non-linear material. These gates rely on two-photon interference of indistinguishable photons. Linear optics quantum computation (LOQC) has the advantage of experimental simplicity. A review can also be found in Kok et al. [Rev. Mod. Phys. 79, 135 (2007)]. Figures 5 and 11-15 are from this review.

As can be seen from Fig. 6 two identical photons impinging on a beam-splitter

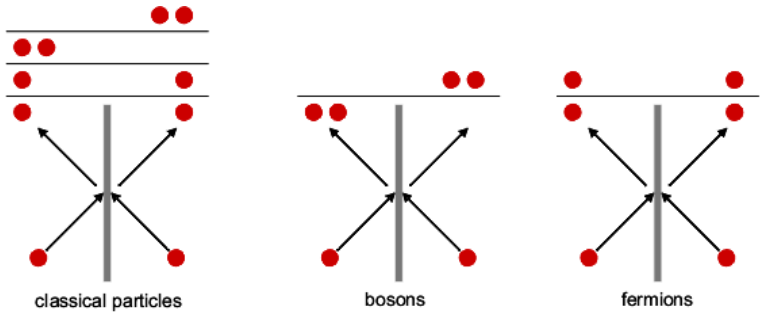

Figure 6: Principle of two-photon interference on a beam-splitter for classical particles, bosons, and fermins

will always leave together. This quantum mechanical effect was first observed by Hong, Ou, and Mandel (Phys. Rev. Lett. 59, 2044 (1987)). Two identical photons were created by parametric down-conversion in a non-linear crystal. The experimental configuration is shown in Fig. 7.

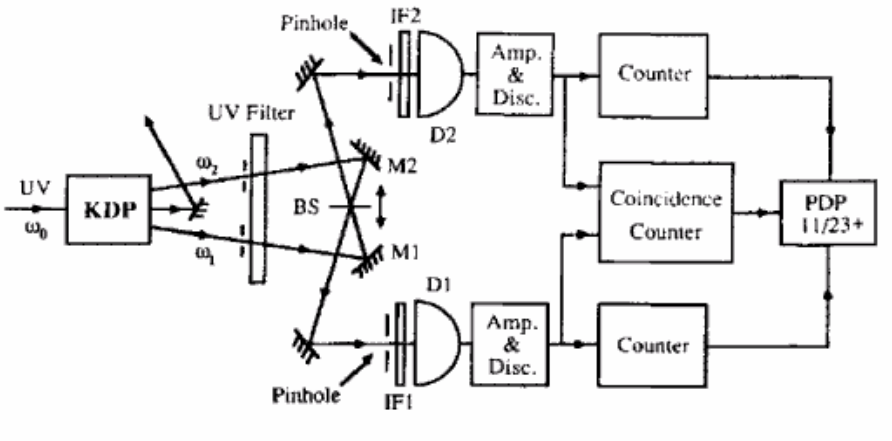

Figure 7: Experimental setup of the Hong-Ou-Mandel experiment [Hong, Ou, and Mandel, Phys. Rev. Lett. 59, 2044 (1987)].

If coincidences or two-photon events are measured as a function of the time of arrival difference at the beam-splitter a pronounced dip is observed, i.e. the two photons never leave on either side, but always together. This dip is called the **Hong-Ou-Mandel dip** or **HOM dip**. Its depth (ideally down to zero) is a measure for the indistinguishability of two photons.

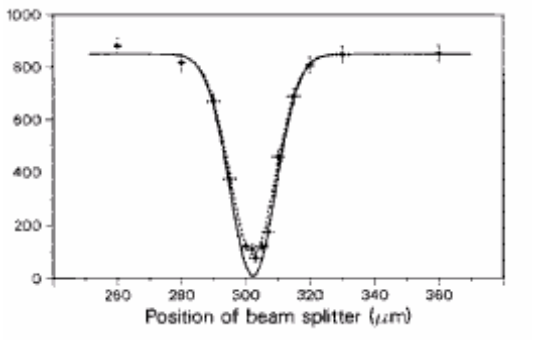

Figure 8: Experimental results of the Hong-Ou-Mandel experiment, the HOM-dip [Hong, Ou, and Mandel, Phys. Rev. Lett. 59, 2044 (1987)].

2.2.2 The KLM-Gate

The HOM interference together with single photon detection can be used to implement two-photon gates. The main idea of the gate proposed by E. Knill, R. Laflamme, and G. J. Milburn (Nature Vol 409, 46 (2001)), the **KLM-gate**, uses so-called ancilla states, which are indistinguishable single photons in additional modes (additional to the qubit modes). After the photons have passed a certain gate made from various optical elements the ancilla states are measured. The operation of the gate is accepted only if a specific outcome is measured. Otherwise the operation has to be started again. Knill et al. proposed a gate NS_{-1} that performs a non-deterministic phase shift on an initial state $|\psi\rangle$ as follows:

$$|\psi\rangle = \alpha_0 |0\rangle + \beta_1 |1\rangle + \gamma_1 |2\rangle = (\alpha_0 + \beta_1 a^\dagger + \gamma_1 a^{(2)\dagger}) |0\rangle \longrightarrow \alpha_0 |0\rangle + \beta_1 |1\rangle - \gamma_1 |2\rangle$$

The gate NS_{-1} can be realized by the network of linear optical elements shown in Fig. 9:

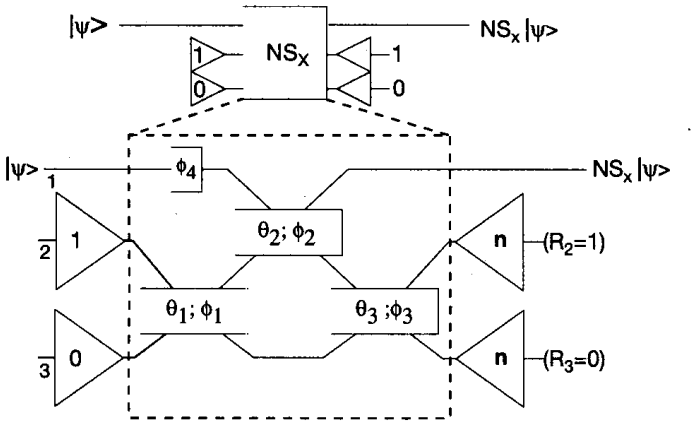

Figure 9: Nonlinear phase shift gate. [from Knill et al., Nature 409, 46 (2001)]

Here the action of each of the three beamsplitters includes a phase shift explicitly, such that e.g. the transformation between the annihilation (creation) operators a_1 and a_2 before and after the beamsplitter is described by the matrix:

$$\begin{pmatrix} \cos\vartheta & -e^{i\phi}\sin\vartheta \\ e^{-i\phi}\sin\vartheta & \cos\vartheta \end{pmatrix}$$

It can be shown that the effect of the whole network for a particular setting of ϑ, and ϕ ($\vartheta_1 = \pi/8, \phi_1 = 0, \vartheta_2 = 3\pi/8, \phi_2 = 0, \vartheta_3 = -\pi/8, \phi_3 = 0, \phi_4 = \pi$) can be described by the following matrix, which transforms the creation (annihilation) operators in modes $1, 2$, and 3:

$$\begin{pmatrix} 1-2^{1/2} & 2^{-1/4} & (3/2^{1/2}-2)^{1/2} \\ 2^{-1/4} & 1/2 & 1/2-1/2^{1/2} \\ (3/2^{1/2}-2)^{1/2} & 1/2-1/2^{1/2} & 2^{1/2}-1/2 \end{pmatrix}$$

At the beginning the ancilla states in mode 2 and 3 are set to:

$$\begin{aligned} |\psi\rangle_2 &= |1\rangle \\ |\psi\rangle_3 &= |0\rangle \end{aligned}$$

The operation is accepted only if the detectors (at R_2 and R_3) measure the ancilla states unchanged, i.e. *exactly* one photon in mode 2 and no photon in mode 3. Otherwise the operation has to start again. The probability of success is $1/4$.

The NS_{-1} gate can then be used to construct a conditional phase shift as illustrated in the following picture:

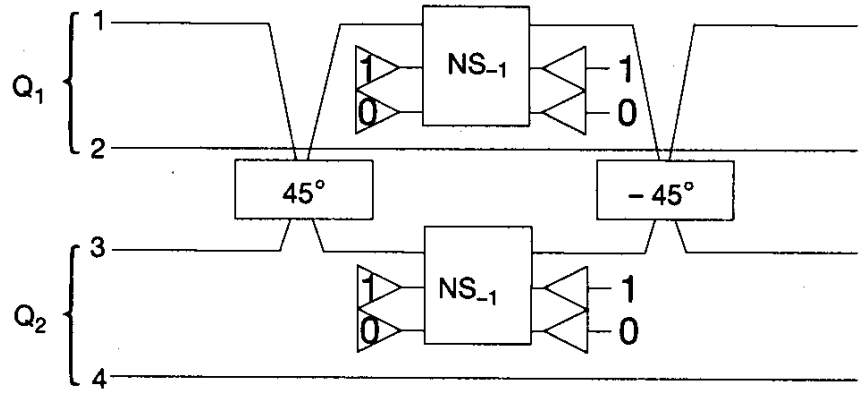

Figure 10: Conditional sign flip gate implemented with NS-1. [from Knill et al., Nature 409, 46 (2001)]

The two beamsplitters set at $45° = \pi/4$ are 50/50 beamsplitters. If exactly one photon is in mode 1 *and* in mode 3 then after the first beamsplitter the state is:

$$|\psi\rangle = |20\rangle_{13} + |02\rangle_{13}$$

Only then a phase shift of -1 occurs which is transferred to qubit Q_2 after the second beam splitter which completes the operation. Thus, the probability of success for the controlled phase shift is 1/16.

One drawback of the proposal is this finite probability. However, in the same paper the authors suggest methods to boost up the success probability arbitrarily close to 1 with the help of even more ancilla states and quantum teleportation. What remains is the requirement for single photon production and for detectors which can discriminate between *zero*, *one*, and *more than one* photon. Additionally, the number of optical elements increases dramatically.

2.2.3 Another intuitive two-photon gate

The KLM proposal motivated many other suggestions for linear optical quantum computing gates. The goal is to reduce the additional effort in terms of the number of ancilla photons and optical elements.

Figure 11 shows another intuitive NS_{-1}-gate proposed by Rudolph and Pan using polarizing beam-splitters (PBS): Assume the input state is horizontally polarized:

$$\left(\alpha + \beta\hat{a}_H^\dagger + \frac{\gamma}{\sqrt{2}}\hat{a}_H^{\dagger 2}\right)\hat{b}_V^\dagger|0\rangle$$

After the first polarizer the state is:

$$\left[\alpha + \beta\cos\sigma\hat{a}_H^\dagger + \beta\sin\sigma\hat{a}_V^\dagger + \frac{\gamma}{\sqrt{2}}(\cos^2\sigma\hat{a}_H^{\dagger 2} + \sin 2\sigma\hat{a}_H^\dagger\hat{a}_V^\dagger + \sin^2\sigma\hat{a}_V^{\dagger 2})\right]\hat{b}_V^\dagger|0\rangle$$

Detecting no photon in the first arm yields:

$$\left(\alpha + \beta\cos\sigma\hat{a}_H^\dagger + \frac{\gamma}{\sqrt{2}}\cos^2\sigma\hat{a}_H^{\dagger 2}\right)\hat{a}_V^\dagger|0\rangle$$

After the second polarizer θ:

$$\left[\alpha + \beta\cos\sigma(\cos\theta\hat{a}_H^\dagger + \sin\theta\hat{a}_V^\dagger) + \frac{\gamma}{\sqrt{2}}\cos^2\sigma(\cos\theta\hat{a}_H^\dagger + \sin\theta\hat{a}_V^\dagger)^2\right]$$

$$\times(-\sin\theta\hat{a}_H^\dagger + \cos\theta\hat{a}_V^\dagger)|0\rangle$$

Finally after detecting a single (!) vertically polarized photon in the second detector:

$$|\psi_{out}\rangle = \alpha\cos\theta|0\rangle + \beta\cos\sigma\cos 2\theta|1\rangle + \gamma\cos^2\sigma\cos\theta(1-\sin^2 3\theta)|2\rangle$$

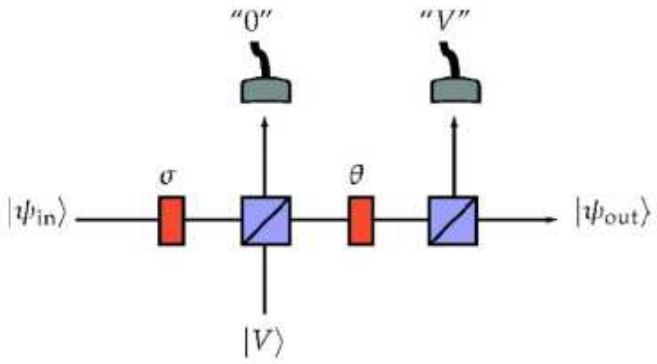

Figure 11: Schematics of the NS_{-1}-gate proposed by Rudolph and Pan

With $\sigma \simeq 150.5°$ and $\theta \simeq 61.5°$ this yields the NS_{-1} gate with probability

$$P_{success} = \cos^2\theta = (3 - \sqrt{2})/7$$

2.2.4 Experimental demonstrations

Several fundamental gates have been demonstrated using LOQC:
Franson et al. Fortschr. Phys. 51, 369 (2003), Fidelity: 86%
O'Brian et al., Nature 426, 264 (2003)], Fidelity: 84%
Pittman et al., Phys. Rev. A 68, 032316 (2003)], Fidelity: 79%
Gasparoni et al., Phys. Rev. Lett. 93, 020504 (2004)], Fidelity: 79%

Usually the gates are tested by measuring the truth table. However, the truth

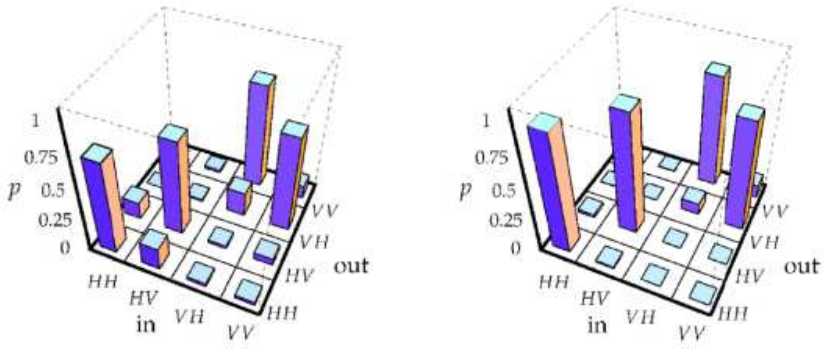

Figure 12: Experimentally obtained truth tables of the gates from Pittman (left) and O'Brian (right)

table in a certain basis is a classical operation. In order to prove the coherence of the gate one has to use coherent superposition of basis states as input. Then, the output state is typically an entangled state. This is shown in the following experimentally determined density matrix of the two photon output state of the gate by O'Brian. For a complete characterization the complete map of all input states to all output states has to be determined.

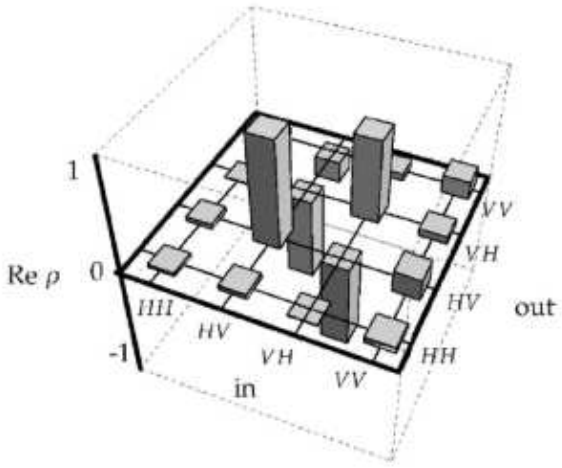

Figure 13: Measured real part of the density matrix of the gate by O'Brian et al. when the input state was a coherent superpositions of the two basis states

2.2.5 Scalability of LOQC

The question may arise if quantum computation with probabilistic gates may be useful at all. When the gates in a computational circuit succeed only with a certain probability p, then the entire calculation that uses N such gates succeeds with probability p^N. The resources time or circuits scale exponentially with the number of gates. In order to do useful quantum computing with probabilistic gates, one has to take the probabilistic elements out of the running calculation. In 1999, Gottesman and Chuang proposed a trick that removes the probabilistic gate from the quantum circuit and places it in the resources that can be prepared offline. It is commonly referred to as the teleportation trick, since it teleports the gate into the quantum circuit.

Suppose a probabilistic CZ gate needs to be applied to two qubits with quantum states $|\phi_1\rangle$ and $|\phi_2\rangle$, respectively. If the gate is applied directly to the qubits, very likely the qubits are destroyed. However, suppose that both qubits are

teleported from their initial mode to a different mode. For one qubit, this is shown in Fig. 14. Here x and z are binary variables, denoting the outcome of the Bell measurement, which determine the unitary transformation that needs to be applied to the output mode. If x=1, the x Pauli operator denoted by X needs to be applied, and if z=1, the z Pauli operator needs to be applied. If x,z=0, no operator has to be applied. For teleportation to work, the entangled resource $|\Phi^+\rangle$ is required, which can be prepared off-line. If a suitable storage device is available, $|\Phi^+\rangle$ does not have to be made on demand: it can be created with a probabilistic protocol using several trials and stored in the storage device.

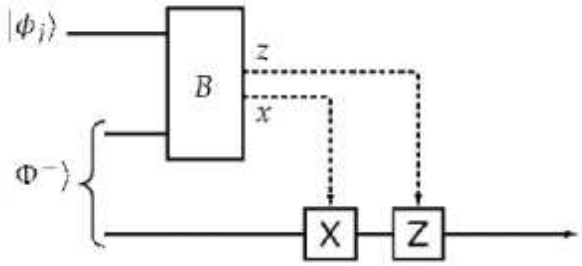

Figure 14: The teleportation circuit. The state $|\phi_j\rangle$ is teleported via a Bell state $|\Phi^+\rangle$ and a Bell measurement B. The binary variables x and z parametrize the outcome of the Bell measurement and determine which Pauli operator is applied to the output mode.

One can now apply the probabilistic CZ gate to the output of two teleportation circuits. Now, the CZ gate can be commuted through the Pauli operators X and Z at the cost of more Pauli operators. That means it can be moved from the right to the left at the cost of only the optically available single-qubit Pauli gates. Again, the required resource can be prepared off-line with a probabilistic protocol and stored in a suitable storage device. There are now no longer any probabilistic elements in the computational circuit.

It is important to note that also teleportation can be implemented with linear optical elements and photon counters, as shown in the KLM proposal. Thus, using these tricks together with efficient error correction LOQC is in principle possible.

In conlcusion, "...the physical resources for the original KLM protocol, albeit scalable, are daunting. For linear optical quantum computing to become a viable technology, we need more efficient quantum gates." [Kok et al., 2007]

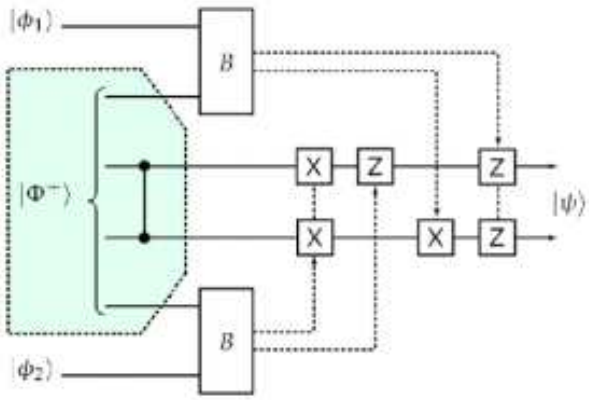

Figure 15: The CZ gate using teleportation: here $|\psi\rangle = U_{CZ}|\phi_1\phi_2\rangle$. By commuting the CZ gate through the Pauli gates from the computational circuit to the teleportation resources, the probabilistic part is taken off-line. The teleportation channel (the shaded area, including the CZ) can be prepared in many trials, without disrupting the quantum computation.

2.2.6 Summary: Optical photon quantum computer

- **Qubit representation:** Location of single photons between two modes $|01\rangle$ and $|10\rangle$, or polarization.
- **Unitary evolution (Kerr media):** Arbitrary transforms are constructed from phase shifters, beam splitters, and non-linear Kerr media. The latter should establish a cross phase modulation of π.
- **Unitary evolution (LOQC):** Single qubit gates are constructed from phase shifters, polarizers, and beam splitters. Two-qubit gates can be constructed with linear optical elements and single photon detectors. Teleportation and efficient error corrections can be implemented to bring the success probability close to unity.
- **Initial state preparation:** Create single photon states. This can be approximated by using attenuated laser light pulses, but for real optical quantum computers single photon states and ancilla states are required.
- **Readout:** Detect single photons, e.g., by an avalanche photo diode (APD).
- **Drawbacks:** Non-linear Kerr media with large ratio of cross phase modulation strength to absorption are difficult to realize.
  LOQC requires huge resources in terms of perfect ancilla states. Also storage media for entangled states are required.

2.3 Cavity Quantum electrodynamics

2.3.1 Jaynes-Cummings-Hamiltonian

In cavity quantum electrodynamics (cavity-QED) one attacks the dilemma of optical quantum computation: On one hand photons seem to be ideal candidates for carrying quantum information. Qubits are relatively easy encoded, and photons only interact weakly with their environment. The latter point however is the main obstacle in order to realize multiple quantum gates. In cavity-QED it is possible to obtain a strong interaction between single atoms and single photons without the problems of scattering, photon loss, or fast decoherence. Single atoms can mediate interactions between two photons and thus cause an effective strong photon-photon interaction.

An important number in cavity-QED is the Q-factor. It is the ratio of the cavity's resonance frequency and its linewidth. The latter is inversely proportional to the photon loss rate. Q-factors exceeding 10^{10} have been realized with photon storage times of seconds. (Compared to acoustic frequencies, say 400 Hz, this would correspond to undamped oscillation of several months!).

The high-Q leads to several important properties:

- The modes have very narrow linewidth. Interaction with single modes can be achieved.
- The photon loss rate is very small and thus decoherence is very small.
- The electromagnetic field is enhanced on resonance. In other words photons are reflected many times from the cavity mirrors or cavity walls. Thus they have the chance to interact many times with atoms in the cavity.
- The latter holds also for the vacuum field which could lead to a strong modification of the spontaneous emission inside the cavity, particularly for cavities with a small mode volume and thus a large electric field per photon

A monochromatic single-mode **electric field** is quantized as follows:

$$\overrightarrow{E}(r) = i\overrightarrow{\varepsilon}E_0\left[ae^{ikr} - a^\dagger e^{-ikr}\right]$$

where E_0 is the amplitude, $\overrightarrow{\varepsilon}$ the polarization, $k = \omega/c$ is the spatial frequency, and $a, a^\dagger$ are the annihilation and creation operators. The free evolution of the field is given by the Hamiltonian:

$$H_{field} = \hbar\omega a^\dagger a$$

The free Hamiltonian of a **two level atom** can be written as:

$$H_{atom} = \frac{\hbar\omega_0}{2}\begin{pmatrix} 1 & 0 \\ 0 & -1 \end{pmatrix} = \frac{\hbar\omega_0}{2}\sigma_3$$

with the Pauli matrix σ_3. The atomic state lives in a two-dimensional Hilbert space and can either be in the lower state with energy E_L or in the upper state with energy E_U. ($\omega_0 = E_U - E_L$).

The **interaction** between atom and field is described as a dipole interaction $\vec{d} \cdot \vec{E}$. Its quantized version in the so-called *rotating wave approximation* is:

$$H_{int} = g(a^\dagger\sigma_- - a\sigma_+)$$

where g is the atom-field coupling constant and σ_-, σ_+ are the Pauli raising and lowering operators:

$$\sigma_+ = \frac{\sigma_1 + i\sigma_2}{2} = \begin{pmatrix} 0 & 1 \\ 0 & 0 \end{pmatrix}, \sigma_- = \frac{\sigma_1 - i\sigma_2}{2} = \begin{pmatrix} 0 & 0 \\ 1 & 0 \end{pmatrix}$$

The **Jaynes-Cummings-Hamiltonian** is the sum of the three Hamiltonians above:

$$H_{JC} = H_{field} + H_{atom} + H_{int} = \hbar\omega a^\dagger a + \frac{\hbar\omega_0}{2}\sigma_3 + g(a^\dagger\sigma_- - a\sigma_+)$$

This Hamiltonian couples the two atomic states $|up\rangle = |1\rangle, |down\rangle = |0\rangle$ with only two photon number states $|n\rangle$ and $|n+1\rangle$. In case of only one excitation (photon) the basis states are: $|0\rangle_{photon}|0\rangle_{atom}, |0\rangle_{photon}|1\rangle_{atom}$, and $|1\rangle_{photon}|0\rangle_{atom}$. In this case the Jaynes-Cummings-Hamiltonian is a 3x3 matrix:

$$H_{JC} = -\begin{pmatrix} \delta & 0 & 0 \\ 0 & \delta & g \\ 0 & g & -\delta \end{pmatrix}$$

where $\delta = (\omega_0 - \omega)/2$ is the detunig and $\hbar = 1$.

It is straightforward to show that the time evolution operator U_{JC} can be written as:

$$\begin{aligned} U_{JC} &= e^{-i\delta t}|00\rangle\langle 00| \\ &+ \left(\cos\Omega t + i\frac{\delta}{\Omega}\sin\Omega t\right)|01\rangle\langle 01| \\ &+ \left(\cos\Omega t - i\frac{\delta}{\Omega}\sin\Omega t\right)|10\rangle\langle 10| \\ &-i\frac{g}{\Omega}\sin\Omega t\,(|01\rangle\langle 10| + |10\rangle\langle 01|) \end{aligned}$$

where $\Omega_R = 2\Omega = \sqrt{\delta^2 + g^2}$ is the *Rabi frequency.*
The dynamics of a two level atom interacting with an electromagnetic field can be represented by a so-called Bloch vector pointing on a Bloch sphere. Here $|0\rangle$ could be the atom in the upper state, and $|1\rangle$ atom in the lower state. With the Bloch vector in the equatorial plane the state is a coherent superposition of the form $1/\sqrt{2}(|0\rangle + e^{i\phi}|1\rangle)$:

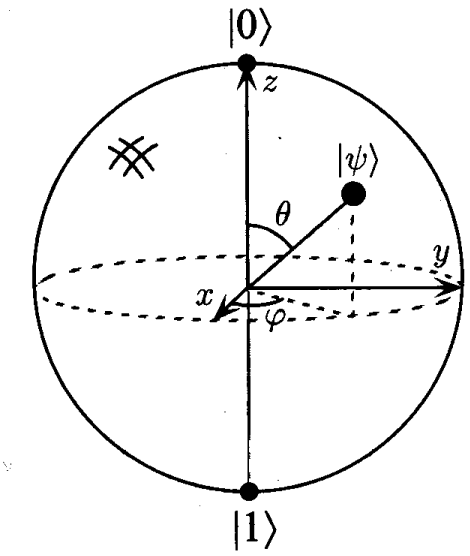

Figure 16: Representation of a qubit state as a vector on a Bloch sphere

2.3.2 Resonant Interaction

As one example the probability that a single photon is absorbed by the atom (initially in the ground state $|0\rangle$) is:

$$p_{absorb} = \sum_k |\langle 0k| U_{JC} |10\rangle|^2 = \frac{g^2}{\delta^2 + g^2} \sin^2 \Omega t = \frac{g^2}{\delta^2 + g^2} \frac{1}{2}(1 - \cos(2\Omega t))$$

Accordingly, the probability to find the atom in the upper state oscillates. This phenomenon is called *Rabi oscillation.* This oscillatory energy exchange between the atom and the field mode is a quantum analog to the classical coupled pendulum problem. It replaces the monotonic and irreversible process of spontaneous emission when an atom interacts with a continuum of modes (e.g. in

free space, see figure below).

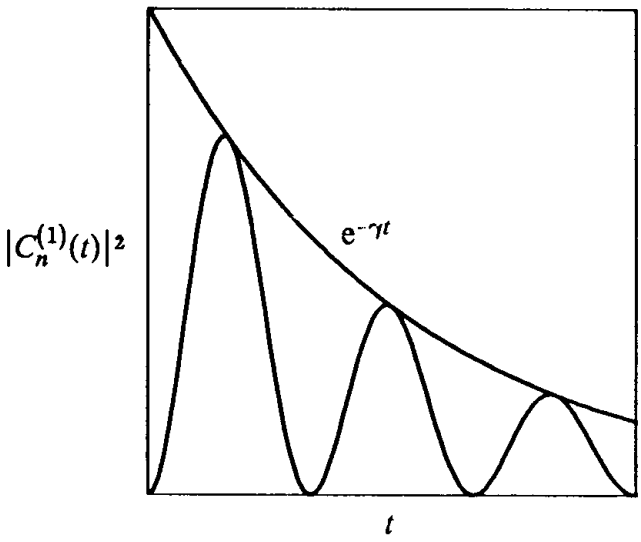

Figure 17: Rabi flopping versus spontaneous decay

Experimental realizations:
First experiments that aimed at the realization of a physical system which could be described by the Jaynes-Cummings Hamiltonian were performed with Rydberg atoms and superconducting resonators. Ryberg atoms are alkali atoms with a single electron in a highly excited state ($n = 50$ to 70). The atoms are thus similar to very large Hydrogen atoms. Since the dipole moment scales with the atoms diameter ($\overrightarrow{d} = \overrightarrow{r} \cdot e$) the interaction of Rydberg atoms with the electromagnetic field is very strong. At the same time their lifetime is very long as well. A transition between two neighboring Rydberg states is a very good approximation for a two level system. These transitions are in the microwave regime (some 10 GHz). Very high-Q superconducting cavities are available for these frequencies.

In the experiments performed in two groups (MPI Garching, and ENS Paris) diluted atomic beams cross different types of cavities (Fabry-Perot or cylinder cavities). The interaction time of the atoms with the field is the time of flight through the cavity. On the average there is at most one atom interacting with the cavity.

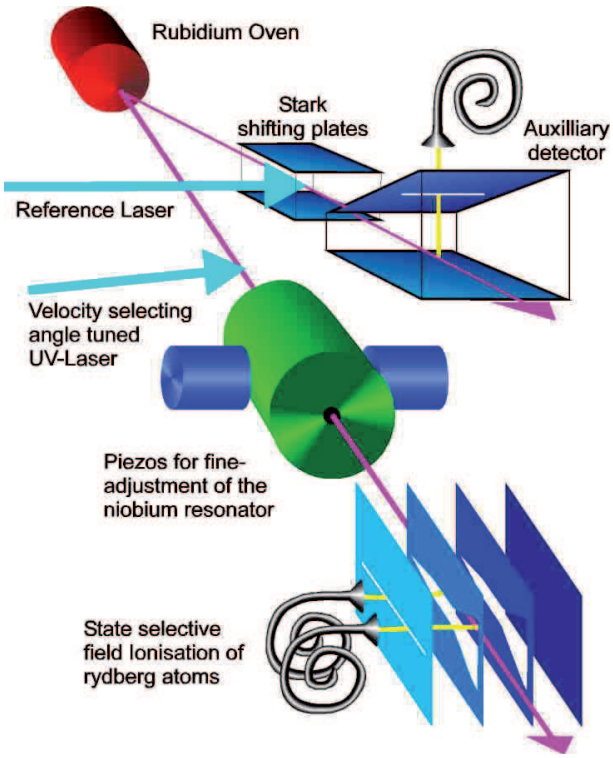

Figure 18: Schematics of the experimental setup in the Garching group (single atom maser). A superconduting microwave cavity is mounted inside a cryostat (also to reduce the number of thermal photons). An atomic oven and laser excitation produces Rydberg states. [from http://www.mpq.mpg.de/micromaser.html]

Single microwave photons cannot be detected. The output of the experiment is encoded in the atoms which have passed the cavity. Atoms which have left the cavity in the upper or lower state an be distinguished by subsequent ionization in an electric field. The detection efficiency is better than 40%.

In the Paris group the Rydberg atoms could be prepared in a coherent superposition of the upper and lower states with the help of a (classical) microwave pulse before entering the cavity. Also, behind the cavity a second microwave pulse acts as an analyzer. In this experiment a rapid tuning (on resonance/off resonance) was possible by applying an electric field between the two cavity mirrors. The resulting Stark effect is strong enough to considerably detune the atom with respect to the cavity. The figures 20 and 21 show experimental

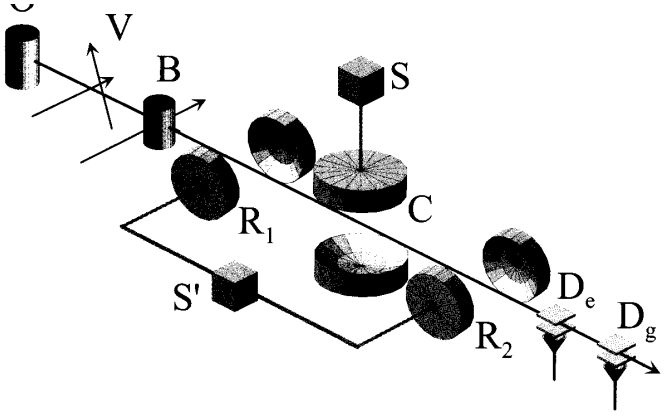

Figure 19: Schematics of the experimental setup in the ENS group in Paris. [from Bouwmeester et al.]

results from the ENS and the Garching group. Both experiments detected Rydberg atoms that had passed an on-resonance cavity. The probability to measure the atoms in the upper or lower state was measured as a function of the time-of-flight through the cavity. In the first experiment a weak coherent state was coupled into the cavity. In the second experiment Fock states were prepared via detection of (one, two, ...) successive Rydberg atoms in the lower state. Then, subsequent atoms detected the according Rabi oscillations.

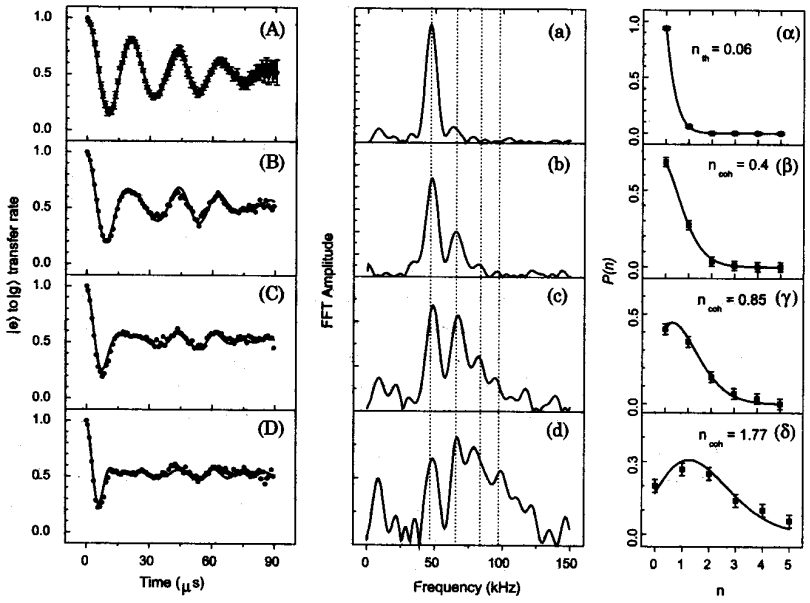

Figure 20: Quantum Rabi oscillations. The probabilty to find an atom in the upper state after passage through the cavity was measured as a function of the time-of-flight. (A), (B), (C), (D) are measurements for increasing field strengths of a coherent state in the cavity, (A) is the vacuum. Middle and left columns are Fourier transforms and calculated photon number distributions. [from Brune et al., M, SchmidtKaler F, Maali A, et al. Phys. rev. Lett., 1800 (1996)]

Another experiment was performed in the ENS group in order to exchange an arbitrary qubit state between two successive atoms. The following sequence was applied

1. Prepare atom 1 in an arbitrary state:

$$|\psi\rangle = (\alpha\,|0\rangle_{atom} + \beta\,|1\rangle_{atom})\,|0\rangle_{field}$$

2. Send atom 1 through the cavity with the cavity in resonance. The interaction time is set such that $\Omega_R t = \pi$, (π-pulse), i.e. an atom in the excited state emits a photon with probability one:

$$\longrightarrow |\psi\rangle = |0\rangle_{atom}\,(\alpha\,|0\rangle_{field} + \beta\,|1\rangle_{field})$$

3. Prepare atom 2 in the ground state:

$$|\psi\rangle' = |0\rangle_{atom}\,(\alpha\,|0\rangle_{field} + \beta\,|1\rangle_{field})$$

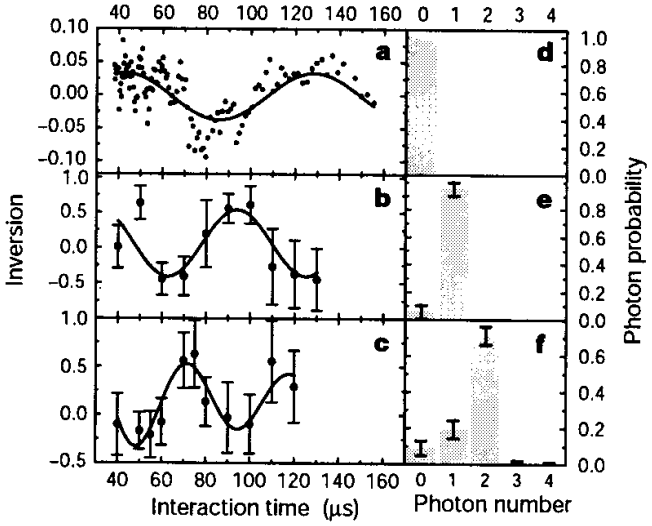

Figure 21: Rabi oscillation after preparation of a n=0, n=1, n=2 Fock state. The normalized difference of the probability to find the atom in the upper or lower state was measured. The left column shows the calculated photon number distribution. [from Varcoe et al., Nature 403, 743 (2000)]

4. Send atom 2 through the cavity with the cavity in resonance. Again the interaction time is set such that $\Omega_R t = \pi$, (π-pulse), i.e. the atom in the ground state absorbs a photon with probability one:

$$\longrightarrow |\psi\rangle' = (\alpha\,|0\rangle_{atom} + \beta\,|1\rangle_{atom})\,|0\rangle_{field}$$

2.3.3 Off Resonant Interaction/Phase Shifts

The phase shift experienced by a single photon due to the presence of a single atom in the ground state can be easily derived from the time evolution operator U_{JC}:

$$\chi_{photon} = \arg\left[e^{-i\delta t}\left(\cos\Omega t - i\frac{\delta}{\Omega}\sin\Omega t\right)\right]$$

For large detuning the absorption of a photon becomes very unlikely, whereas there is still a considerable phase shift.

Similarly the phase shift experienced by an atom in the ground state due to the presence of one photon is:

$$\chi_{atom} = \arg\left[\cos\Omega t - i\frac{\delta}{\Omega}\sin\Omega t\right]$$

The phase shift of the atomic ground state due to the presence of a single photon can be used to realize a *conditional phase shift gate*. Such a gate can be used to construct a universal two qubit logic gate.

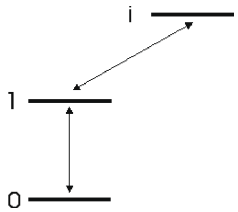

Figure 22: Schematics of the levels used for experimental realization of a conditional phase gate

Control and target qubit are encoded in two successive atoms. The experimental procedure goes as follow:

1. Prepare atom 1 (control) in a coherent superposition:

$$|\psi\rangle = \frac{1}{\sqrt{2}}(|0\rangle_{atom} + |1\rangle_{atom})\,|0\rangle_{field}$$

2. Send atom 1 through the cavity with the cavity *in resonance* with respect to the $0 \longrightarrow 1$ transition (see Fig. 22), i.e. swap the atomic state to the photon state:

$$\longrightarrow |\psi\rangle = |0\rangle_{atom}\,\frac{1}{\sqrt{2}}(|0\rangle_{field} + |1\rangle_{field})$$

3. Prepare atom 2 (target) in a coherent superposition:

$$|\psi\rangle' = \frac{1}{\sqrt{2}}(|0\rangle_{atom} + |1\rangle_{atom})\frac{1}{\sqrt{2}}(|0\rangle_{field} + |1\rangle_{field})$$

4. Send atom 2 through the cavity with the cavity *off resonance* or in resonance with a $2\pi-$pulse condition with respect to the $1 \longrightarrow i$ transition

(see Fig. 22):

$$\begin{aligned} \longrightarrow \quad & |\psi\rangle' = \frac{1}{2}(|0\rangle_{atom} + |1\rangle_{atom})\,|0\rangle_{field} + \frac{1}{2}(|0\rangle_{atom} + e^{i\chi}\,|1\rangle_{atom})\,|1\rangle_{field} \\ = \quad & \frac{1}{2}(|00\rangle + |10\rangle + |01\rangle + e^{i\chi}\,|11\rangle) \end{aligned}$$

The shift χ depends on the detuning of the $1 \longrightarrow i$ transition. In case of zero detuning a photon can be absorbed by the 1 state. In this case the interaction time is set such that $\Omega_R t = 2\pi$, (2π-pulse), i.e. the atom absorbs a photon but emits it again with probability one. Thus the state of the 1 state of atom remains unchanged and only experiences a phase shift of $\chi = -1$.

The following shows experimental results of a conditioned-phase gate achieved in the ENS experiment:

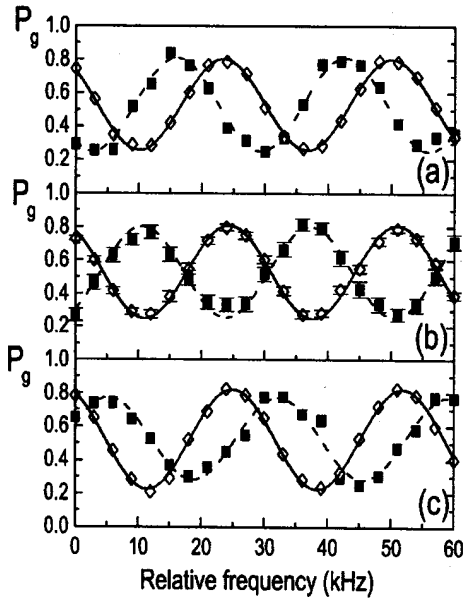

Figure 23: Experimental results of a conditioned-phase gate. The probability to detect the atom in in the ground state is measured for various cavity detunings. Open diamonds correspond to an empty cavity, solid squares are single photon fringes. [from Rauschenbeutel et al., Phys. Rev. Lett. 83, 5166]

2.3.4 Flying Qubits

A single atom can mediate the interaction between two photons very effectively. It can be regarded as an almost ideal Kerr medium to achieve cross-phase modulation. The most fundamental system to study the Kerr effect consists of a single three level atom interacting with two modes of the electromagnetic field:

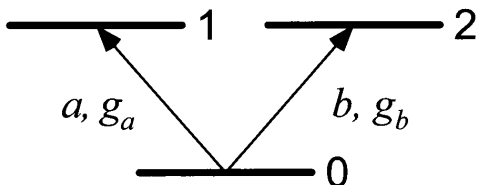

Figure 24: Model of a three level system as a Kerr medium

For such a system (with degenerate energy levels 1 and 2) the generalized Jaynes-Cummings Hamiltonian is:

$$H_{JC} = \sum_{i=1,2} \hbar\omega a_i^\dagger a_i + \frac{\hbar\omega_0}{2}\sigma_3 + \sum_{i=a,b} g_i(a_i^\dagger \sigma_{i-} - a_i\sigma_{i+})$$

It can be shown that a single photon in mode a or mode b experiences a phase shift ϕ_a and ϕ_b if an atom in the ground state is present. This phase shift could be understood classically by the index of refraction of the atom in the cavity. However, there is an additional phase shift Δ if both photons are present. The non-linear phase shift is plotted in the following figure depending on the atom-cavity detuning. This additional phase shift is the Kerr cross phase modulation.

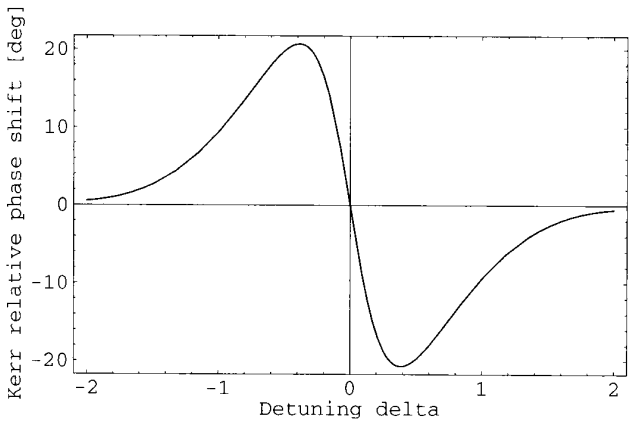

Figure 25: Calculated Kerr shift of a three level atom as afunction of the atom cavity detuning [from Nielsen and Chuang]

An experiment where a conditional phase shift gate with the help of the Kerr effect was realized was performed in the group of Kimble at Caltech, USA. In contrast to the experiment in the ENS group the qubits were encoded in two single photons (flying qubits) in two modes. The photonic qubit states were approximated by two weak coherent states in two orthogonal modes with slightly different frequencies.

The initial state was a linearly polarized (probe) beam and a circularly polarized (pump) beam:

$$\begin{aligned} |\psi\rangle_{in} &= |\beta^+\rangle_{pump} \frac{1}{\sqrt{2}}(|\alpha^+\rangle + |\alpha^-\rangle)_{probe} \\ &\approx \left[|0^+\rangle + \beta\,|1^+\rangle\right] \frac{1}{\sqrt{2}} \left[|0^+\rangle + \alpha\,|1^+\rangle + |0^-\rangle + \alpha\,|1^-\rangle\right] \end{aligned}$$

Here the +,- denotes left or right circular polarization. The atom was a Cs atom optically pumped in the $6S_{1/2}, F = 4, m_F = 4$ state.

After the atom had interacted with the cavity the photons were left in the state:

$$\begin{aligned} |\psi\rangle_{out} &\approx |0^+\rangle \frac{1}{\sqrt{2}} \left[|0^+\rangle + \alpha e^{i\phi_a}\,|1^+\rangle + |0^-\rangle + \alpha\,|1^-\rangle\right] \\ &\quad + \beta e^{i\phi_b}\,|1^+\rangle \frac{1}{\sqrt{2}} \left[|0^+\rangle + \alpha e^{i(\phi_a+\Delta)}\,|1^+\rangle + |0^-\rangle + \alpha\,|1^-\rangle\right] \end{aligned}$$

The states in square brackets are linearly polarized states which are tilted off the vertical by an angle ϕ_a and $\phi_a + \Delta$, respectively. The shift of the probe beam was detected in the experiment with the help of a balanced homodyne detector (the local oscillator discriminated the pump from the probe beam).

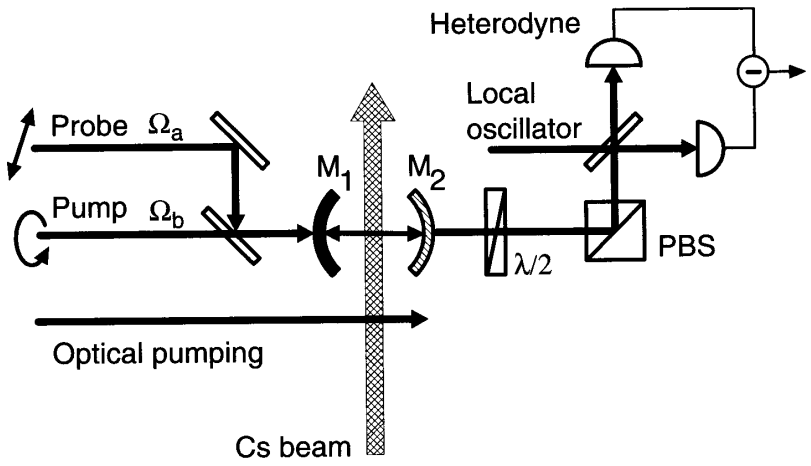

Figure 26: Experimental demonstration of a conditional phase gate in the Caltech experiment. Qubits were encoded in photons ("flying qubits"), a strong Kerr nonlinearity was mediated by single Cs atoms. [from Turchette et al. Phys. Rev. Lett. 75,4710 (1995)]

In the experiment the shifts.$\phi_a = 17.5°$, $\phi_b = 12.5°$, and $\Delta = 16°$ were established. This experiment thus demonstrates the possibility to realize a universal two qubit quantum gate.

More recent experiments with high-Q cavities are performed in the optical domain. In these experiments atomic traps instead of atomic beams are used. Atoms are trapped and cooled above a cavity and then dropped. This increases the interaction time. However, it is extremely difficult to cascade many cavities. First results have also been obtained with semiconductor nanostructures (quantum dots) in solid-state cavities [Yoshie et al., Nature 432, 200 (2004); Reithmaier et al., Nature 432, 197 (2004); Peter et al., Phys. Rev. Lett. 95, 067401 (2005)]. Rabi oscillations could be observed. These all-solid state systems may have the potential for up-scaling towards two, three, N (?) quantum dots and/or cavities.

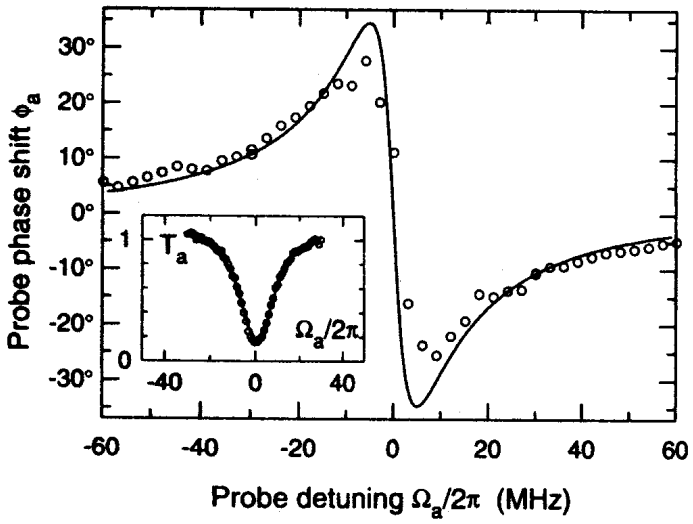

Figure 27: Measured phase shift in the Caltech experiment. The mean number of atoms in the cavity was 1. The inset shows the transmission of the probe through the cavity. [from Turchette et al. Phys. Rev. Lett. 75,4710 (1995)]

2.3.5 Summary: Cavity QED implementation of quantum computers

- **Qubit representation:** Location of single photons between two modes $|01\rangle$ and $|10\rangle$, or polarization.
- **Unitary evolution:** Arbitrary transforms are constructed from phase shifters, beam splitters, and cavity QED systems.
- **Initial state preparation:** Create single photon states. This can be approximated by using attenuated laser light pulses.
- **Readout:** Detect single photons, e.g. by an avalanche photo diode (APD).
- **Drawbacks:** The coupling of two photons is mediated by a atom. Thus a strong atom field coupling is desirable. Coupling of photons into and out of the cavity then becomes difficult. The scalability is limited.